The Astrophysical Journal, 577:680–690, 2002 October 1

THE BRIGHT GAMMA-RAY BURST OF 2000 FEBRUARY 10: A CASE STUDY OF AN OPTICALLY DARK GAMMA-RAY BURST

L. Piro,[1] D. A. Frail,[2] J. Gorosabel,[3,4] G. Garmire,[5] P. Soffitta,[1] L. Amati,[6] M. I. Andersen,[7] L. A. Antonelli,[8] E. Berger,[9] F. Frontera,[6,10] J. Fynbo,[11] G. Gandolfi,[1] M. R. Garcia,[12] J. Hjorth,[13] J. in 't Zand,[14] B. L. Jensen,[13] N. Masetti,[6] P. Møller,[11] H. Pedersen,[13] E. Pian,[15] and M. H. Wieringa[16]

Received 2002 January 16; accepted 2002 June 8

ABSTRACT

The gamma-ray burst GRB 000210 had the highest gamma-ray peak flux of any event localized by *BeppoSAX* as yet, but it did not have a detected optical afterglow, despite prompt and deep searches down to $R_{\rm lim} \approx 23.5$. It is therefore one of the events recently classified as dark GRBs, whose origin is still unclear. *Chandra* observations allowed us to localize the X-ray afterglow of GRB 000210 to within $\approx 1''$, and a radio transient was detected with the Very Large Array. The precise X-ray and radio positions allowed us to identify the likely host galaxy of this burst and to measure its redshift, $z = 0.846$. The probability that this galaxy is a field object is $\approx 1.6 \times 10^{-2}$. The X-ray spectrum of the afterglow shows significant absorption in excess of the Galactic one corresponding, at the redshift of the galaxy, to $N_{\rm H} = (5 \pm 1) \times 10^{21}$ cm^{-2}. The amount of dust needed to absorb the optical flux of this object is consistent with the above H I column density, given a dust-to-gas ratio similar to that of our Galaxy. We do not find evidence for a partially ionized absorber expected if the absorption takes place in a giant molecular cloud. We therefore conclude that either the gas is local to the GRB but is condensed in small-scale high-density ($n \gtrsim 10^9$ cm^{-3}) clouds, or the GRB is located in a dusty, gas-rich region of the Galaxy. Finally, we examine the hypothesis that GRB 000210 lies at $z \gtrsim 5$ (and therefore that the optical flux is extinguished by Lyα forest clouds), but we conclude that the X-ray–absorbing medium would have to be substantially thicker from that observed in GRBs with optical afterglows.

Subject headings: cosmology: observations — gamma-rays: bursts

1. INTRODUCTION

It is observationally well established that about half of the accurately localized gamma-ray bursts (GRBs) do not produce a detectable optical afterglow (Frail et al. 2000; Fynbo et al. 2001), while most of them ($\approx$90%) have an X-ray afterglow (Piro 2001). Statistical studies have shown that the optical searches of these events, known variously as "dark GRBs," "failed optical afterglows" (FOAs), or "gamma-ray bursts hiding an optical source transient" (GHOSTs), have been carried out to magnitude limits fainter on average than the known sample of optical afterglows (Lazzati, Covino, & Ghisellini 2002; Reichart & Yost 2001; but see also Fynbo et al. 2001). Some of these GRBs could be intrinsically faint events, but this fraction should not be very high, because the majority of dark GRBs show the presence of an X-ray afterglow similar to that observed in GRBs with optical afterglows (Piro 2001; Lazzati et al. 2002). Thus, dark bursts could constitute a distinct class of events and not just be the result of an inadequate optical search, but it is unclear whether this observational property derives from a single origin or is a combination of different causes.

If the progenitors of long-duration GRBs are massive stars (Paczyński 1998), as current evidence suggests (e.g., Bloom et al. 1999; Piro et al. 2000), extinction of optical flux by dusty star-forming regions is likely to occur for a substantial fraction of events (the obscuration scenario). Another possibility is that dark GRBs are located at redshift $z \gtrsim 5$, with the optical flux being absorbed by the intervening Lyα forest clouds (the high-redshift scenario).

Dark bursts that can be localized to arcsecond accuracy, through a detection of either their X-ray or radio afterglow, are of particular interest. The first and best-studied example was GRB 970828, for which prompt, deep searches down to $R \sim 24.5$ failed to detect an optical afterglow (Odewahn et al. 1997; Groot et al. 1998), despite the fact that it was

[1] Istituto Astrofisica Spaziale and Fisica Cosmica, CNR, Via Fosso del Cavaliere, 00133 Rome, Italy.
[2] National Radio Astronomy Observatory, Socorro, NM 87801.
[3] Danish Space Research Institute, Juliane Maries Vej 30, DK-2100 Copenhagen Ø, Denmark.
[4] Instituto de Astrofísica de Andalucía, CSIC, Apartado Correos 3004, 18080 Granada, Spain.
[5] Department of Astronomy and Astrophysics, 525 Davey Lab, Pennsylvania State University, University Park, PA 16802.
[6] Istituto Astrofisica Spaziale and Fisica Cosmica, Sezione Bologna, CNR,Via Gobetti 101, 40129 Bologna, Italy.
[7] Division of Astronomy, University of Oulu, P.O. Box 3000, FIN-90014, Finland.
[8] Osservatorio Astronomico Roma, INAF, Via Frascati 33, 00040 Monte Porzio Catone, Rome, Italy.
[9] California Institute of Technology, Palomar Observatory 105-24, Pasadena, CA 91125.
[10] Dipartimento Fisica, Università Ferrara, Via Paradiso 12, Ferrara, Italy.
[11] European Southern Observatory, Karl-Schwarzschild-Strasse 2, D-85748 Garching, Germany.
[12] Harvard-Smithsonian Center for Astrophysics, 60 Garden Street, Cambridge, MA 02138.
[13] Astronomical Observatory, University of Copenhagen, Juliane Maries Vej 30, DK-2100 Copenhagen Ø, Denmark.
[14] Space Research Organization in the Netherlands, Sorbonnelaan 2, 3584 CA Utrecht, The Netherlands.
[15] Osservatorio Astronomico Trieste, INAF, Via G. Tiepolo 11, I-34131 Trieste, Italy.
[16] Paul Wild Observatory, Locked Bag 194, Narribri NSW 2390, Australia.

localized within a region of only 10″ radius by the *ROSAT* satellite (Greiner et al. 1997). Djorgovski et al. (2001) recently showed how the detection of a short-lived radio transient for GRB 970828 allowed them to identify the probable host galaxy and to infer its properties (redshift, luminosity, and morphology). In addition, they used estimates of the column density of absorbing gas from X-ray data and lower limits on the rest-frame extinction ($A_V > 3.8$) to quantify the amount of obscuration toward the GRB.

Given the extreme luminosity of GRBs and their probable association with massive stars, it is expected that some fraction of events will be located beyond $z > 5$ (Lamb & Reichart 2000). These would be probably classified as dark bursts, because the UV light, which is strongly attenuated by absorption in the Lyα forest, is redshifted into the optical band. Fruchter (1999) first suggested such an explanation for the extreme red color of the optical/NIR emission for GRB 980329, although an alternative explanation based on H_2 absorption in the GRB environment would imply a somewhat lower redshift (Draine 2000). In a recent paper, Jaunsen et al. (2002) derived a photometric redshift $z \approx 3.5$. We note that the three redshifts determined or suggested so far for dark GRBs ($z = 0.96$, GRB 970828; Djorgovski et al. 2001; $z = 1.3$, GRB 990506; Taylor et al. 2000; Bloom et al. 2002; $z \approx 0.47$, GRB 000214; Antonelli et al. 2000) are in the range of those measured for most bright optical afterglows, but whether this applies to the majority of these events is still to be assessed. Particularly interesting in this respect is the case of the so-called X-ray flashes or X-ray–rich GRBs discovered by *BeppoSAX* (Heise et al. 2001). In most of these events, no optical counterpart has been found. The only tentative association claimed as yet is for the event of 2001 October 30, in which a candidate host galaxy of magnitude $V \approx 25$ has been found in the direction of the afterglow (Fruchter et al. 2002). We note, however, that the probability that this object is a foreground galaxy is not negligible ($P \approx 3 \times 10^{-2}$; see, e.g., eq. [2] in § 2.3). The high-redshift scenario would naturally explain both the absence of an optical counterpart and the high-energy spectrum, because the peak of the gamma-ray spectrum would be redshifted into the X-ray band.

If we are to use dark bursts to study obscured star formation in the universe (Djorgovski et al. 2001), we must first understand the source of the extinction. For those afterglows that are not at $z > 5$, it is important to establish whether they are dark because of a dense circumburst medium (Reichart & Yost 2001) or because their optical emission is extinguished by line-of-sight absorption from the medium of the host galaxy. We can use the properties of the afterglow, its location within the host galaxy, and the properties of the host galaxy itself to address this question. In this paper, we report observations of the burst GRB 000210, which was discovered and localized by *BeppoSAX*. A *Chandra* observation of the *BeppoSAX* error box enabled us to localize the likely host galaxy of the event and identify a short-lived radio transient, further refining the position to subarcsecond accuracy. From sensitive upper limits on the absence of an optical afterglow, we estimate the amount of extinction by dust, and from the X-ray spectrum, we estimate the amount of absorbing gas. GRB 000210 appears to be the newest member of a small but growing group of well-localized dark bursts (Frail et al. 1999; Taylor et al. 2000; Djorgovski et al. 2001).

2. OBSERVATIONS

2.1. *Gamma-Ray and X-Ray Observations*

The gamma-ray burst GRB 000210 was detected simultaneously by the *BeppoSAX* Gamma-Ray Burst Monitor (GRBM) and Wide-Field Camera 1 (WFC) on 2000 February 10, 08:44:06 UT. As of now, this event is the brightest GRB detected simultaneously by the GRBM and WFC, with a peak flux $F(40\text{–}700\ \mathrm{keV}) = (2.1 \pm 0.2) \times 10^{-5}$ ergs cm^{-2} s^{-1}, ranking in the top 1% of the BATSE catalog. In X-rays, the event was also very bright, with a peak flux $F(2\text{–}10\ \mathrm{keV}) = (1.5 \pm 0.2) \times 10^{-7}$ ergs cm^{-2} s^{-1}, ranking fourth after GRB 990712 (Frontera et al. 2001), GRB 011121 (L. Piro et al. 2002, in preparation), and GRB 01022 (in't Zand et al. 2001). The gamma-ray light curve shows a FRED-like[17] pulse (Fig. 1), with a duration of about 15 s. The X-ray light curve shows a longer pulse, with a tail persisting for several tens of seconds. The fluence $(40\text{–}700\ \mathrm{keV}) = (6.1 \pm 0.2) \times 10^{-5}$ ergs cm^{-2} ranks GRB 000210 in the top five brightest GRBs seen by the GRBM and WFC, and in the top 3% of the BATSE bursts (Kippen et al. 2000). With an $F(2\text{–}10\ \mathrm{keV})/F(40\text{–}700\ \mathrm{keV}) = 0.007$, GRB 000210 is one of the hardest GRBs detected by *BeppoSAX* (Feroci et al. 2001). The spectrum is also very hard in the X-ray band. Time-resolved spectra of the WFC, fitted with a power-law model $F = Ce^{-\sigma N_{\mathrm{H}}} E^{-\Gamma}$, give $\Gamma = (0.38 \pm 0.13)$ and $\Gamma = (0.82 \pm 0.12)$ in the rising and first decaying part of the peak, with the usual hard-to-soft evolution continuing in the subsequent parts, with $\Gamma = 2.3 \pm 0.15$ for $18\ \mathrm{s} < t < 80\ \mathrm{s}$ (Fig. 1). The absorption column density is consistent with that in our Galaxy ($N_{\mathrm{H},G} = 2.5 \times 10^{20}$ cm^{-2}), with an upper limit $N_{\mathrm{H}} \lesssim 2 \times 10^{22}$ cm^{-2}.

The GRB was localized with the WFC at (epoch J2000) R.A. $= 01^{\mathrm{h}}59^{\mathrm{m}}14\overset{\mathrm{s}}{.}9$, decl. $= -40°40\overset{\prime}{.}14$ within a radius of 2′. This position is consistent with the Interplanetary Network (IPN) annulus derived by *Ulysses*, Konus, and the *BeppoSAX*/GRBM (Hurley et al. 2000). Prompt dissemination of the coordinates (Gandolfi et al. 2000a, 2000b; Stornelli et al. 2000) triggered follow-up observations by several ground-based and space observatories, including *BeppoSAX* and *Chandra*. A *BeppoSAX* target-of-opportunity observation (ToO) started on February 10.66 UT (7.2 hr after the GRB) and lasted until February 11.98 UT. Net exposure times were 44 ks for the MECS and 15 ks for the LECS. The X-ray fading afterglow was detected (Costa et al. 2000) within the WFC error circle at (epoch J2000) R.A. $= 01^{\mathrm{h}}59^{\mathrm{m}}15\overset{\mathrm{s}}{.}9$, decl. $= -40°39'29''$ (error radius $= 50''$; see Fig. 2). The X-ray flux from the source exhibited a decay consistent with the standard power-law behavior, with $F(2\text{–}10\ \mathrm{keV}) = 3.5 \times 10^{-13}$ ergs cm^{-2} s^{-1} in the first 30 ks of the observation (Fig. 3). The spectrum derived by integrating over the entire observation is well fitted by a power law with photon index $\Gamma = 1.75 \pm 0.3$, column density $N_{\mathrm{H}} < 4 \times 10^{21}$ cm^{-2}, consistent with that in our Galaxy and flux $F(2\text{–}10\ \mathrm{keV}) = 2.2 \times 10^{-13}$ ergs cm^{-2} s^{-1}.

The *Chandra* ToO started approximately 21 hr after the burst (i.e., around the middle of the *BeppoSAX* ToO), with an exposure time of 10 ks with ACIS-S with no gratings. The X-ray afterglow was near the center of the *BeppoSAX* NFI region (Fig. 2). The initial position (Garcia et al.

[17] Fast rise, exponential decay.

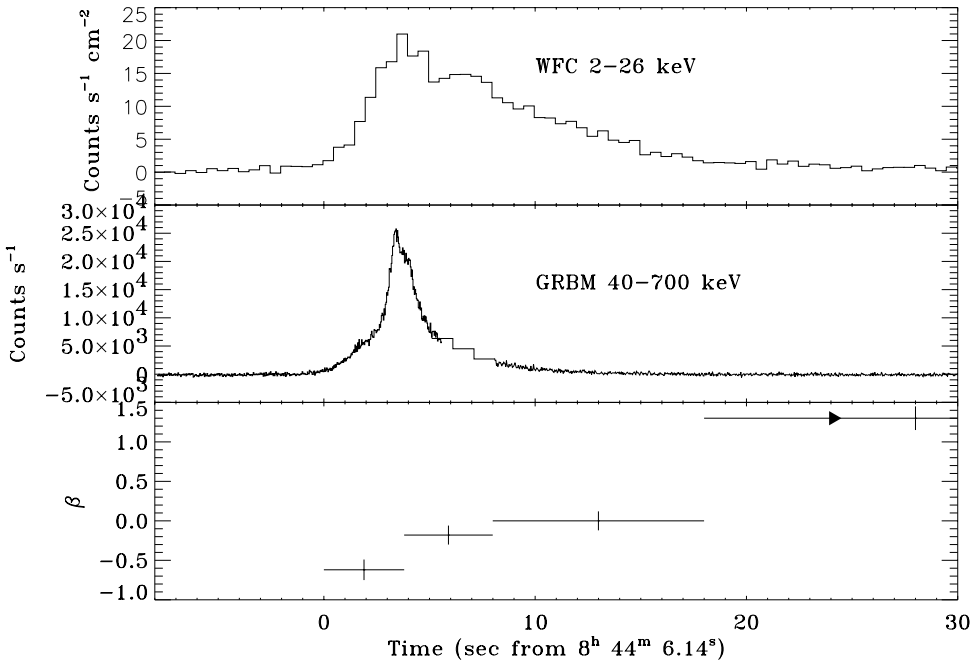

FIG. 1.—Light curves of GRB 000210 in the *BeppoSAX* WFC (*top panel*), GRBM (*middle panel*), and energy spectral index ($\beta = \Gamma - 1$, $F \propto E^{-\beta}$) evolution in the WFC (*bottom panel*). The gap between 5.5 and 8 s in the GRBM data is due to a telemetry loss. In that interval, we have plotted the 1 s resolution data of the ratemeter of the instrument, while the other data points have a time bin of 31.25 ms. The last point of the spectral index is relative to the interval 18–80 s.

2000b) derived from the first data processing by the *Chandra* X-Ray Center was found to be affected by an aspect error of about 8″ (Garcia, Garmire, & Piro 2000a). Reprocessing of the data with the correct attitude calibration solved this problem (Garmire et al. 2000). We have further improved this position, following the prescription suggested by the *Chandra* team,[18] using five stars detected in X-rays and comparing their positions to the USNO-A2.0 and Two Micron All Sky Survey (2MASS) catalog positions. The final position of the GRB is (epoch J2000) R.A. = $01^h59^m15^s.58$, decl. = $-40°39'33''.02$, with an estimated error radius of 0″.6 (90% confidence level).

The ACIS-S total counts were 555 ± 26, corresponding to $F(2\text{–}10\ \text{keV}) = 1.8 \times 10^{-13}$ ergs cm $^{-2}$ s $^{-1}$ for a best-fit power law ($\chi^2 = 20.9$ with 22 degrees of freedom [dof]) with index $\Gamma = 2.0 \pm 0.2$ and a significant amount of absorption $N_{\rm H} = (0.17 \pm 0.04) \times 10^{22}$ cm^{-2}, well above that expected from our Galaxy.

We have performed a simultaneous fit to the *Chandra* ACIS-S and *BeppoSAX* MECS and LECS data with an absorbed power law, leaving the relative normalization of the instruments free, to account for the nonsimultaneous coverage of the decaying source. The resulting fit (Fig. 4) is satisfactory ($\chi^2/\text{dof} = 26/34$). In particular, the ACIS-S/MECS relative normalization is 1.08 ± 0.2, and $\Gamma = 1.95 \pm 0.15$. In the inset of Figure 4, we present the confidence levels of the intrinsic hydrogen column density as a function of the redshift of the source.

In Figure 3, we plot the light curve in the 2–10 keV range from the prompt emission to the afterglow. Frontera et al. (2000) have argued that *on average*, the afterglow starts at a time ≈60% of the duration of the burst. This is consistent with what we observe in GRB 000210. The steep gradient of the WFC light curve flattens out around $t = 20$ s, suggesting that at this time the afterglow starts dominating over the prompt emission. In fact, the WFC data points at $t \gtrsim 20$ s and the *BeppoSAX* and *Chandra* data follow a power-law decay ($F \propto t^{-\alpha_{\rm X}}$) with $\alpha_{\rm X} = 1.38 \pm 0.03$ and $F(2\text{–}10\ \text{keV}, t = 11\ \text{hr}) = 4 \times 10^{-13}$ ergs cm^{-2} s^{-1}. This interpretation is also supported by the spectral behavior, with the WFC spectral index attaining a value of $\Gamma = (2.3 \pm 0.15)$ around $t = 20$ s, consistent with that observed at later times by the *BeppoSAX* NFI and *Chandra* ACIS-S.

There is no evidence for a break in the X-ray light curve, which would have been clearly detected if present in such a bright burst (e.g., GRB 990510; Pian et al. 2001; GRB 010222; in 't Zand et al. 2001).

2.2. *Optical Observations*

We obtained optical imaging of the field of GRB 000210 with the 2.56 m Nordic Optical Telescope (NOT) equipped with the High Resolution Adoptive Camera (HiRAC) and with the 1.54 m Danish Telescope (1.54D) plus the Danish Faint Object Spectrograph and Camera (DFOSC), starting 12.4 and 16 hr after the burst, respectively. Further observations were carried out in 2000 August and October. A log of these observations can be found in Table 1, while in Table 2 we list the secondary standards used for the calibration of the optical magnitudes of the field.

The observations (Fig. 5) revealed a faint extended object located within the *Chandra* error circle (Gorosabel et al. 2000). The contours of the optical emission (Fig. 6) show that the source is slightly elongated in the northeast direction with an angular extension of ∼1″.5. The angular size in the orthogonal direction (northwest) is limited by the seeing (0″.7 in our best images). The center of the object (i.e., excluding the diffuse component) has coordinates (epoch J2000) R.A. = $01^h59^m15^s.61$, decl. = $-40°39'33''.1$, with a

[18] See http://asc.harvard.edu/mta/ASPECT/.

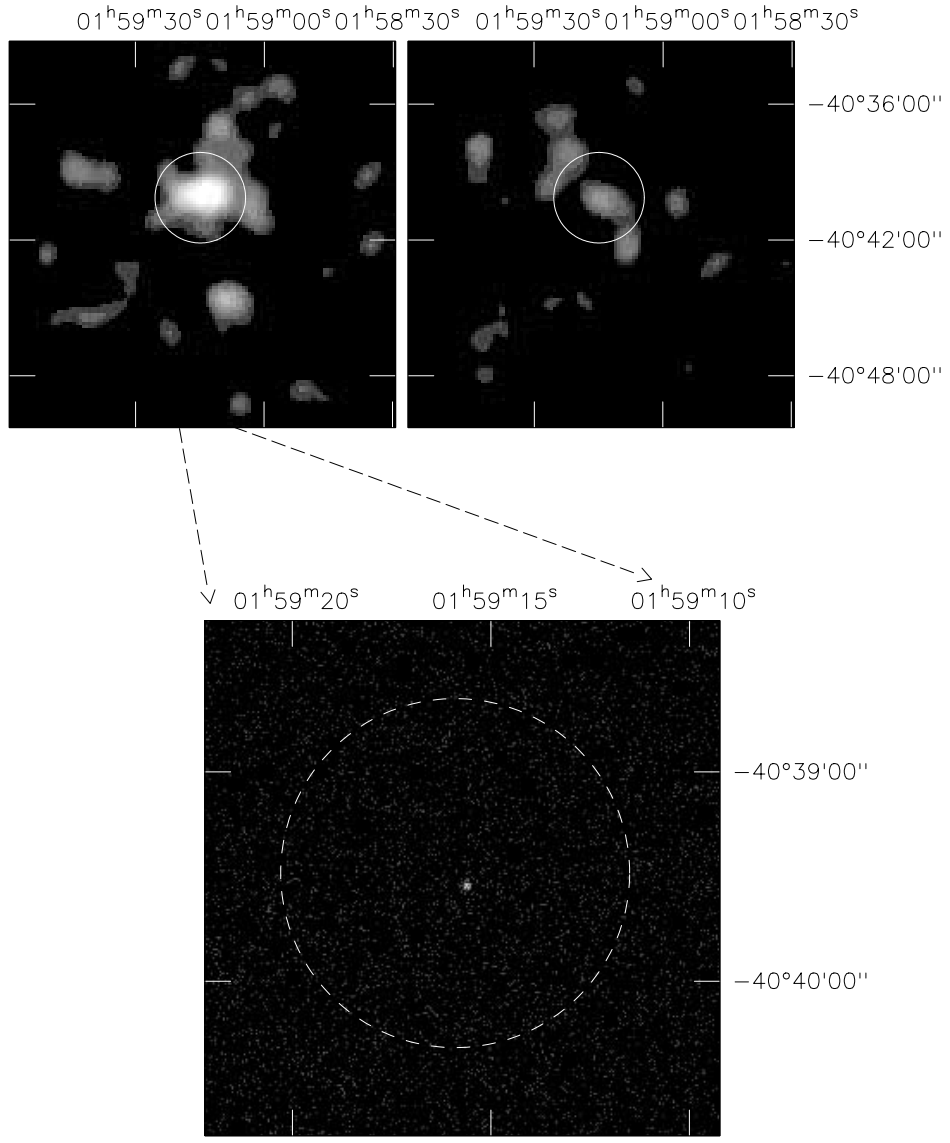

FIG. 2.—Image of the X-ray afterglow of GRB 000210 by *BeppoSAX* and *Chandra*. *Top panel*: Left and right images show the afterglow in the *BeppoSAX* MECS (1.6–10 keV) 8 and 30 hr after the GRB, respectively. The circle represents the WFC error box. *Bottom panel*: *Chandra* ACIS-S (0.2–8 keV) image of the afterglow 21 hr after the GRB. The dashed circle is the *BeppoSAX* NFI error box.

90% uncertainty of 0.″74, which represents the sum in quadrature of a systematic error of 0.″4 and a statistical error of 0.″6. This position is the mean value of astrometric calibrations on three independent images based on the USNO-A2.0 catalog. The position of two of the stars detected in the *Chandra* image, which are included in the smaller field of view of the optical image, demonstrates that the optical and X-ray fields are tied to within ≈0.″2 (90% confidence level). A comparison of early and late observations shows that the object remains constant in brightness within the photometric errors, with magnitudes $B = 25.1 \pm 0.7$, $V = 24.1 \pm 0.15$, $R = 23.5 \pm 0.1$, and $I = 22.60 \pm 0.12$. Although the object in Figure 6 is very faint, its appearance is not stellar.

2.3. *The Host Galaxy?*

Spectroscopic observations confirmed that the object is a galaxy. The observations were carried out on 2000 October 25 with the Very Large Telescope (VLT1) equipped with the Focal Reducer Spectrograph (FORS1). The 300V grism and the 0.″7 slit provided a spectral FWHM resolution of ∼10 Å. The spectrum is based on a single 2000 s exposure and covers the range between 4193 and 8380 Å. The reduction is based on standard procedures, i.e., flat-field correction with internal lamp flats and wavelength calibration using arc lamps. No spectrophotometric standard stars were observed, so no flux calibration was possible.

The spectrum revealed an emission line at 6881.2 ± 0.5 Å, $\sim 6\,\sigma$ above the continuum level (Fig. 7). Given the presence of a well-detected continuum blueward of the line and the absence of other emission lines in the 4193–8380 Å range, we identify this line with the 3727 Å [O II] line at a redshift of $z = 0.8463 \pm 0.0002$. The equivalent width of the line is EW $= (68 \pm 9)$ Å. We stress that the absence of V dropout in photometric data, expected by Lyα forest absorption at high z, indicates by itself that $z < 4$ (Madau 1995).

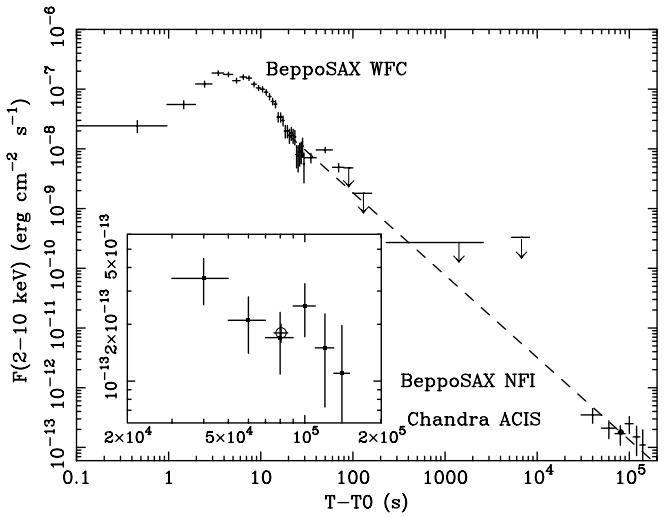

FIG. 3.—Light curve from *BeppoSAX* WFC (from 0.1 to 5000 s), and *BeppoSAX* NFI and *Chandra* ACIS (from 30.000 to 140.000 s). The latter data are expanded in the inset. The *Chandra* data point is identified by an open circle.

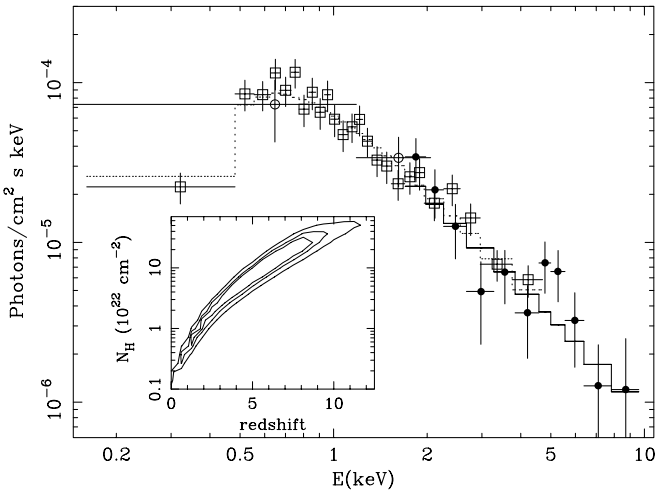

FIG. 4.—X-ray spectrum of the afterglow by *BeppoSAX* LECS (*open circles*), MECS (*filled circles*), and *Chandra* ACIS-S (*open squares*). The continuous (*dashed*) line is the best-fit absorbed power law to the *BeppoSAX* (*Chandra*) data. The contour plot of the intrinsic absorption column density as a function of the redshift is plotted in the inset. The contours correspond to 68%, 90%, and 99% confidence level (*thin, normal, and thick lines*, respectively).

Is this galaxy the *host* of GRB 000210? We have computed the probability of a chance association in two ways. First, we have computed the probability of finding an unrelated field galaxy with $R < R_{\rm host} = 23.5$ within the localization circle of the afterglow (1″ radius, i.e., the 99% *Chandra* error radius). From galaxy counts (Hogg et al. 1997), we derive that $P = 10^{-2}$. A slightly more conservative estimation is given by the fraction of the sky covered by galaxies brighter than $R_{\rm host}$,

$$P = \int^{R_{\rm host}} A(m)\frac{dN}{dm}\,dm, \qquad (1)$$

where dN/dm is the mean number of galaxies per magnitude per unit solid angle and $A(m)$ is the average area of a galaxy of R-band magnitude m. For $m > 21$ $dN/dm \approx 10^{0.334m}$ (Hogg et al. 1997), while for brighter galaxies $dN/dm \approx 10^{0.5m}$ (Koo & Kron 1992). We have estimated the average area of a galaxy $A = \pi(2r_{\rm hl})^2$, where $r_{\rm hl}$ is the half-light radius of the galaxy. We have adopted the following empirical half-light radius-magnitude relations: $r_{\rm hl} = 0\farcs6 \times 10^{-0.075(m-21)}$, for $21 < m < 27$ (Odewhan et al. 1996; Bloom et al. 2002), and $r_{\rm hl} = 0\farcs6 \times 10^{-0.2(m-21)}$ for brighter galaxies (Im et al. 1995, and references therein). By substituting these relations in equation (1), we derive

$$P = [4.9 + 3.8 \times 10^{0.184(R_{\rm host}-21)}] \times 10^{-3}, \quad 21 < R_{\rm host} < 27. \qquad (2)$$

For $R_{\rm host} = 23.5$, $P = 1.6 \times 10^{-2}$. Therefore, a chance association is unlikely but not completely negligible.

TABLE 1
OPTICAL OBSERVATIONS OF GRB 000210

Epoch (UT)	Filter	Exposure Time (s)	Seeing (arcsec)	Telescope[a]	Magnitude
Feb 10.88–10.90	*R*	3 × 300	1.2	NOT	>23
Feb 11.03–11.08	*R*	10 × 300	1.6	1.54D	23.5 ± 0.2
Feb 14.02–14.03	*R*	600	1.9	1.54D	>22.6
May 5.42–5.44	*R*	2 × 600	2.3	1.54D	>22
Aug 22.29–22.41	*R*	7 × 900	2.2	1.54D	23.47 ± 0.10
Aug 23.23–23.29	*R*	5 × 900	2.3	1.54D	23.47 ± 0.10
Aug 24.23–24.30	*R*	4 × 900	3.0	1.54D	23.47 ± 0.10
Aug 26.29–26.43	*V*	9 × 900	1.5	1.54D	24.09 ± 0.15
Aug 27.21–27.24	*I*	2 × 900	1.4	1.54D	22.60 ± 0.12
Aug 28.21–28.24	*I*	2 × 1200	1.4	1.54D	22.60 ± 0.12
Aug 29.21–29.30	*I*	7 × 1200	1.1	1.54D	22.60 ± 0.12
Aug 30.22–30.24	*I*	1200	1.1	1.54D	22.60 ± 0.12
Aug 31.21–31.24	*B*	2 × 1200	1.5	1.54D	25.1 ± 0.7
Oct 25.24–25.24	*R*	300	0.7	VLT	23.46 ± 0.10

NOTE.—*R* and *I* magnitudes from August 22 to 24 and from August 27 to 30 have been derived by summing the images obtained in those nights.

[a] NOT: Nordic Optical Telescope; 1.54D: 1.54 m Danish Telescope; VLT: Very Large Telescope.

TABLE 2
POSITIONS AND MAGNITUDES OF THE SECONDARY STANDARDS REPORTED IN FIGURE 5

ID	α_{J2000}	δ_{J2000}	I	R	V	B	U
1.....	01 59 10.056	−40 37 15.11	17.21 ± 0.02	17.71 ± 0.02	18.20 ± 0.02	19.01 ± 0.03	19.64 ± 0.08
2.....	01 59 17.877	−40 37 20.58	16.51 ± 0.02	16.91 ± 0.02	17.26 ± 0.02	17.81 ± 0.03	17.88 ± 0.05
3.....	01 59 16.762	−40 37 51.37	15.93 ± 0.02	17.00 ± 0.02	18.00 ± 0.02	19.40 ± 0.03	20.71 ± 0.12
4.....	01 59 12.370	−40 37 57.60	18.09 ± 0.03	19.15 ± 0.03	20.18 ± 0.03	21.54 ± 0.04	23.11 ± 0.25
5.....	01 59 04.478	−40 38 19.70	17.34 ± 0.02	17.64 ± 0.02	17.86 ± 0.02	18.16 ± 0.03	17.99 ± 0.06
6.....	01 59 06.665	−40 38 21.51	16.07 ± 0.02	16.52 ± 0.02	16.89 ± 0.02	17.47 ± 0.03	17.49 ± 0.04
7.....	01 59 16.673	−40 40 20.09	16.60 ± 0.02	16.74 ± 0.02	16.78 ± 0.02	16.83 ± 0.02	17.07 ± 0.03

NOTE.—Units of right ascension are hours, minutes, and seconds, and units of declination are degrees, arcminutes, and arcseconds.

2.4. *Radio Observations*

Very Large Array (VLA)[19] observations were initiated within 15 hr after the burst. Details of this and all subsequent VLA observations are given in Table 3. In addition, a single observation was also made two days after the burst with the Australian Telescope Compact Array (ATCA).[20] All VLA observations were performed in standard continuum mode, with a central frequency of 8.46 GHz, using the full 100 MHz bandwidth obtained in two adjacent 50 MHz bands. The flux density scale was tied to the extragalactic source 3C 48 (J0137+331), while the phase was monitored using the nearby source J0155−408. The ATCA observation was made at a central frequency of 8.7 GHz, with a 256 MHz bandwidth obtained in two adjacent 128 MHz bands. The flux density scale was tied to the extragalactic source J1934−638, while the phase was monitored using the nearby source J0153−410.

[19] The NRAO is a facility of the National Science Foundation operated under cooperative agreement by Associated Universities, Inc. NRAO operates the VLA.

[20] The Australia Telescope is funded by the Commonwealth of Australia for operation as a National Facility managed by CSIRO.

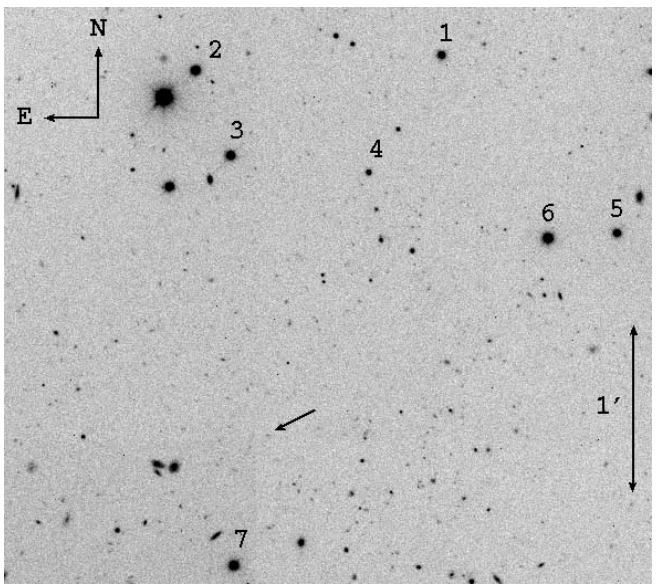

FIG. 5.—*R*-band VLT image of the GRB 000210 field. The numbers label the secondary standards (Table 2).

On 2000 February 18.95 UT, a radio source was detected within the *Chandra* error circle with a peak brightness of 99 ± 21 μJy beam^{-1}, or a flux density (after Gaussian fitting) of 93 ± 21 μJy. The synthesized beam was $6'' \times 2''$, with a position angle on the sky of 30° counterclockwise. The position of this source is (epoch J2000) R.A. = $01^h59^m15^s.57$ ($\pm 0^s.05$), decl. = $-40°39'31''.9$ ($\pm 1''.0$), where the errors are at 90% confidence level in the Gaussian fit. We have further refined the astrometry by looking for coincident USNO-2.0 stars. We find one radio source coincident with a star, shifted by an offset of ($-0^s.05$, $0''.56$) in R.A. and decl. Taking into account this offset, we derive the final position of the radio counterpart of the GRB at R.A. = $01^h59^m15^s.62$, decl. = $-40°39'32''.46$. The position of this radio transient is in excellent agreement with the X-ray afterglow and the optical source (Fig. 6). The transient nature of this source is readily apparent (see Table 3), since it was not detected in observations either before or after February 18.

3. DISCUSSION

3.1. *Properties of the Host*

In the following, we assume a cosmology with $H_0 = 65$ km s^{-1} Mpc^{-1}, $\Omega_m = 0.3$, and $\Omega_\Lambda = 0.7$. At $z = 0.846$, the luminosity distance $D_L = 1.79 \times 10^{28}$ cm, and $1''$ corresponds to 8.3 proper kpc in projection. The gamma-ray fluence implies an isotropic gamma-ray energy release $E_\gamma = 1.3 \times 10^{53}$ ergs.

The [O II] 3727 line flux can be used to estimate the star formation rate (SFR) of the galaxy (Kennicutt 1998). Although the spectrum has not been calibrated, we have derived a rough estimation of the line flux by rescaling the line flux measured in the host galaxy of GRB 970828 for the line EW, R magnitudes, and redshifts (Djorgovski et al. 2001). We find $L_{3727} \approx (1\text{–}2) \times 10^{41}$ ergs s^{-1}, corresponding to SFR $\approx 3\ M_\odot$ yr^{-1}. Since we are not sensitive to any obscured components of SFR, this relatively modest SFR is only a lower limit to the true star-forming rate. From the I-band photometry, we derive a rest-frame absolute magnitude $M_B = -19.9 \pm 0.1$, corresponding to a $\approx 0.5 L_*$ galaxy today (Schechter 1976). The location of the afterglow is within $\approx 1''$ the center of the Galaxy, corresponding to about 8 kpc in projection.

3.2. *The Nature of the Obscuring Medium*

The *Chandra* and *BeppoSAX* observations detected an X-ray afterglow that clearly underwent a power-law decay with $\alpha_X = 1.38 \pm 0.03$. There is no evidence for a temporal

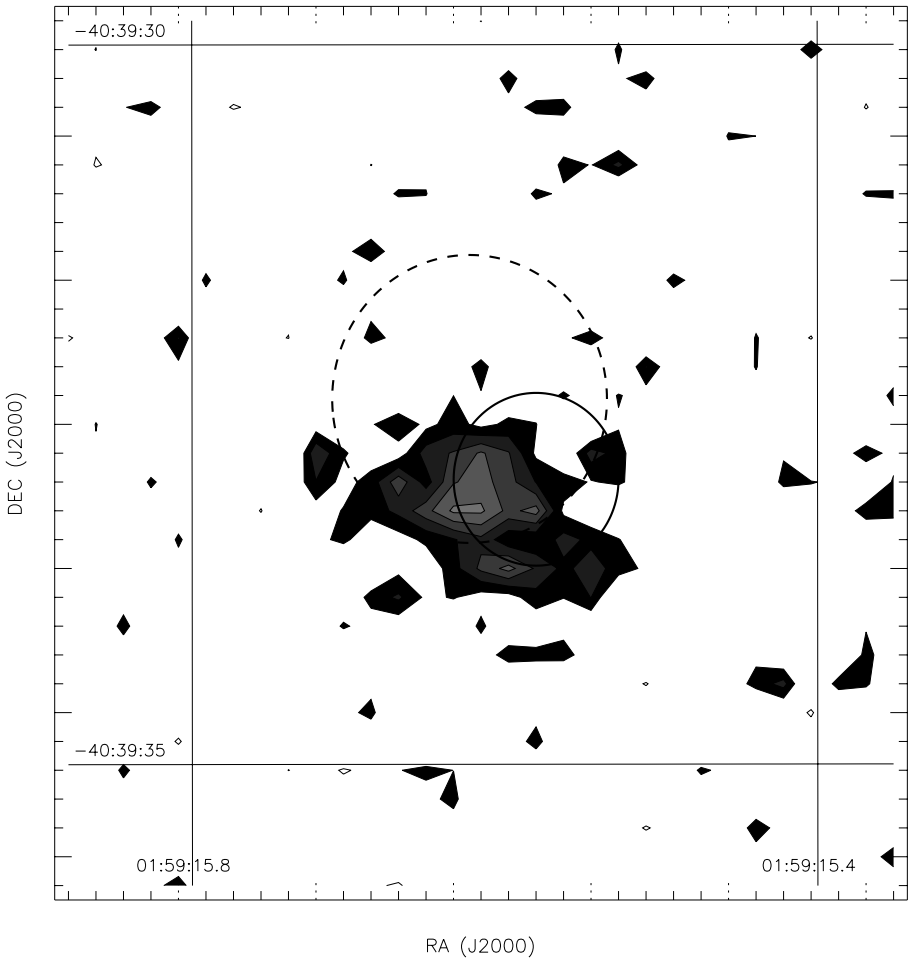

FIG. 6.—Blow-up of Fig. 5, showing the contour plot of the likely host galaxy of GRB 000210. The circles show the 90% error circles of the *Chandra* (*solid line*) and radio (*dashed line*) afterglows.

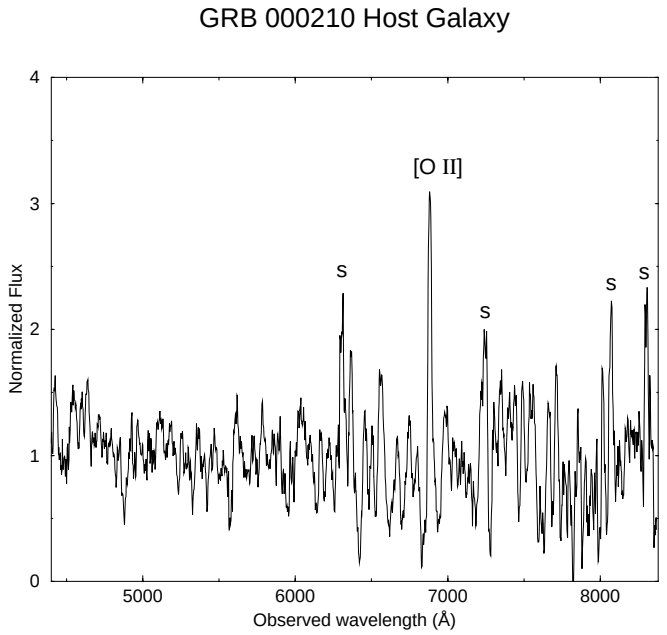

FIG. 7.—Normalized spectrum of the GRB 000210 host galaxy acquired with VLT+FORS1. The spectrum has been smoothed with a boxcar width corresponding to the instrumental spectral resolution (10 Å). The spikes, mostly present in the red part of the spectrum and indicated with an "S," are residuals from the subtraction of strong sky emission lines. The region of the [O II] line is not affected by sky emission lines.

break in the X-ray light curve between 10 and 2×10^5 s after the burst (Fig. 3). A deviation from a power-law decay could occur if the synchrotron cooling break ν_c passed through the band, or the outflow began to exhibit jet geometry, or at the transition to nonrelativistic expansion. In all respects, the X-ray afterglow of GRB 000210 was fairly typical in comparison with past events (Piro 2001).

The VLA and ATCA measurements indicate that the only significant detection of the radio afterglow from GRB 000210 was 9 days after the burst. With an 8.46 GHz flux density of 93 ± 21 μJy, this is the weakest radio afterglow detected to date. The time interval between the burst and the radio peak is too long to be the result of a reverse shock propagating in the relativistic ejecta (Kulkarni et al. 1999; Sari & Piran 1999). It is more likely that the emission originated from a forward shock that reached a maximum on this timescale (e.g., Frail et al. 1999). Interstellar scintillation can briefly increase (or decrease) the radio flux of a weak afterglow and make it detectable (Goodman 1997; Waxman, Kulkarni, & Frail 1998). With these single-frequency measurements, it cannot be determined whether the 8.46 GHz flux density was weak because GRB 000210 was a low-energy event or because the synchrotron self-absorption frequency was high ($\nu_{\rm ab} > 10$ GHz). Reichart & Yost (2001) have argued that a high $\nu_{\rm ab}$ is expected for dark bursts if they occur in dense circumburst environments ($n \gg 10^2$ cm^{-3}).

TABLE 3
RADIO OBSERVATIONS OF GRB 000210

Epoch (UT) (1)	Δt (days) (2)	ν (GHz) (3)	Telescope (4)	Array (5)	$S \pm \sigma$ (μJy) (6)
2000 Feb 10.98	0.62	8.46	VLA	B	34 ± 70
2000 Feb 12.32	1.96	8.70	ATCA	6A	-4 ± 59
2000 Feb 14.90	4.54	8.46	VLA	B	15 ± 37
2000 Feb 15.03	4.67	8.46	VLA	CnB	-34 ± 42
2000 Feb 18.95	8.59	8.46	VLA	CnB	93 ± 21
2000 Feb 26.95	16.59	8.46	VLA	CnB	20 ± 16
2000 Mar 3.92	21.56	8.46	VLA	CnB	58 ± 33
2000 Mar 27.81	45.45	8.46	VLA	C	45 ± 45
2000 May 28.73.....	107.37	8.46	VLA	C	48 ± 26
2000 Jun 24.69.....	134.33	8.46	VLA	D	-1 ± 34

NOTE.—Col. (1): UT date for each observation. Col. (2): Time elapsed since the gamma-ray burst. Col. (3): Observing frequency. Col. (4): Telescope name. Col. (5): Array configuration. Col. (6): Peak flux density at the best-fit position of the radio transient, with the error given as the rms noise in the image.

Although the X-ray and radio afterglow were detected for GRB 000210, there are only lower limits for the magnitude of the expected optical transient of $R > 22$ and 23.5 at 12.4 and 16 hr after the burst, respectively. Following Djorgovski et al. (2001), we can use the fireball model to predict the expected optical flux and then derive a lower limit to the amount of the extinction. The simplest model of an isotropic fireball expanding into a constant density medium is assumed (Sari et al. 1998). This assumption is well justified, since all well-studied afterglows are better explained by expansion in a constant density medium rather than in a wind-shaped one (Panaitescu & Kumar 2001). For the timescales of interest ($t < 21$ hr), there is no evidence for a break in the X-ray light curve that would indicate a jetlike geometry or transition to nonrelativistic expansion. Two limiting cases are considered. The first is when the cooling frequency ν_c lies below the optical band ν_o (i.e., $\nu_c < \nu_o$). The expected optical spectral flux density is $f_o = f_{\rm X}(\nu_o/\nu_{\rm X})^{-p/2}$, where $f_{\rm X}$ is the X-ray spectral flux density at $\nu_{\rm X}$. In the second case, the cooling frequency lies between the optical and X-ray bands (i.e., $\nu_o < \nu_c < \nu_{\rm X}$). There is a local minimum when $\nu_{\rm X} \simeq \nu_c$ and, consequently, the expected optical spectral density is $f_o = f_{\rm X}(\nu_o/\nu_{\rm X})^{-(p-1)/2}$. As long as $\nu_c \leq \nu_{\rm X}$, the electron energy spectral index $p = (2/3 + 4/3\alpha_{\rm X}) = 2.51 \pm 0.04$. This value of p is also consistent with the spectral slope measured in X-rays.

The X-ray flux measured by *Chandra* 21 hr after the burst was $F(2\text{–}10\ \text{keV}) = 1.8 \times 10^{-13}$ ergs cm^{-2} s^{-1}, which corresponds to a spectral flux density $f_{\rm X} = 0.01$ μJy at 4 keV [adopting $\beta_{\rm X} = (\Gamma - 1) = 0.95 \pm 0.15$, where $f_{\rm X} \propto \nu^{-\beta_{\rm X}}$]. For $\nu_c < \nu_o$, the predicted optical magnitudes are therefore $R \sim 17.4$ and 17.7 at 12.4 and 16 hr after the burst, respectively. The equivalent magnitudes for the case $\nu_o < \nu_c \simeq \nu_{\rm X}$ are $R \sim 21.5$ and 21.9. Taking the more stringent limits on the absence of an optical transient 21 hr after the burst, we infer significant extinction toward GRB 000210, with a range of upper limits lying between $A_R = 1.6$ and 5.8 mag. Using the extinction curve as formulated by Reichart (2001a), we convert these A_R limits from the observer frame to a rest-frame extinction of $A_V = 0.9\text{–}3.2$ (for $z = 0.85$) and derive a hydrogen equivalent column density $N_{{\rm H},o} \gtrsim (0.2\text{–}0.6) \times 10^{22}$ cm^{-2}, assuming the Galactic relation of Predehl & Schmitt (1995).

How does this result compare with the estimate of absorption derived from the X-ray data? In Figure 4, we show the contour plot of the X-ray column density in the GRB frame as a function of the redshift, under the assumption that the absorbing material is in a neutral cold state. At $z = 0.85$, the absorption is $N_{\rm H,X} = (0.5 \pm 0.1) \times 10^{22}$ cm^{-2}. Thus, $N_{\rm H,X}/N_{{\rm H},o}$ is consistent with unity, or less, and therefore the dust-to-gas ratio is compatible with that of our Galaxy, as it has also been found in the other dark GRB 970828 (Djorgovski et al. 2001). In contrast, Galama & Wijers (2000) noted that a number of bursts with optical afterglows seem to exhibit large column density as inferred from X-ray afterglow data, but with little or no optical extinction, suggesting that GRBs destroy dust grains along the line of sight. Different authors (Waxman & Draine 2000; Fruchter et al. 2001; Reichart 2001b) present mechanisms by which dust in the circumburst medium is destroyed or depleted by the light from the optical flash and X-rays from the burst and early-time afterglow up to a distance $R \approx 10 L_{49}^{1/2}$ pc ($L = 10^{49} L_{49}$ ergs s^{-1} is the isotropic-equivalent luminosity of the optical flash). Reichart (2001b) and Reichart & Price (2002) proposed a unified scenario to explain the two populations of GRBs. They argue that most GRBs occur in giant molecular clouds (GMCs), with properties similar to those observed in our Galaxy (size $\approx$20–90 pc; Solomon et al. 1987). Assuming that the energy reservoir is standard (Frail et al. 2001; Piran et al. 2001), strongly collimated bursts would burn out completely through the clouds, thus producing a detectable optical afterglow, regardless of the column density through the cloud. Weakly collimated bursts would not destroy all the dust, leaving a residual column density through the line of sight. If this column density is sufficiently high, optical photons of the afterglow will be extinguished, making a dark GRB.

We find, however, that this scenario is not consistent with the observed properties of the X-ray absorber, if GRB 000210 lies at $z = 0.846$. For typical densities of a GMC ($n \approx 10^2\text{–}10^5$ cm^{-3}), the gas should be ionized by GRB photons on scales of several parsecs (Boettcher et al. 1999; Lazzati & Perna 2002). Over the whole cloud, the medium would span a wide range of ionization stages, from fully ionized to neutral, with a substantial fraction of the gas being in partially ionized stages. We have verified this case by fit-

ting the *BeppoSAX* and *Chandra* spectra with an ionized absorber (model *absori* in XSPEC) at redshift $z = 0.85$. The ionization stage is described by the ionization parameter $\xi = L_X/nR^2$, where R is the distance of the gas from the GRB. We do not find any evidence of an ionized absorber, with a tight upper limit of $\xi < 1$. In fact, even a moderate level of ionization would result in a reduced opacity below $\approx$1 keV, due to the ionization of light elements such as C and O, but this feature is not observed in the X-ray spectrum.

3.2.1. *High-Density Clouds*

We have shown that in the GMC scenario, the X-ray–absorbing gas is expected to be substantially ionized, contrary to what is observed. We now introduce a variation of the local absorption scenario, in which a phase of the medium is condensed in high-density clouds or filaments with low filling factor. We show that this scenario is consistent with the properties of the X-ray absorption.

To keep the gas in a low-ionized stage at a distance of the order of a few pc, a density $n \gtrsim 10^9$ cm^{-3} is required. In fact, the recombination timescale $t_{\rm rec} \approx n^{-1}T^{-0.5}$, where T is the electron temperature. In the case of iron, $t_{\rm rec} = 300 n_9^{-1} T_7^{-0.5}$ s (i.e., Piro et al. 2000; hereafter, given a quantity X, we define $X_n = 10^{-n}X$). The typical temperature is expected to be in the range $T_7 \approx 0.1$–1 (Piro et al. 2000; Paerels et al. 2000). Therefore, at sufficiently high density, recombination is effective in keeping the gas close to ionization equilibrium over timescales $\gtrsim t_{\rm rec}$, i.e., during the afterglow phase. The ionization parameter is then $\xi = L_{45}/n_9 R_{18}^2$, where $L_{45} = 3$ is the luminosity of the X-ray afterglow in the rest-frame energy range 0.013–100 keV. For $n_9 \gtrsim 1$, the medium is then in the neutral phase for distances $R_{18} \gtrsim 1$, as required. It is straightforward to show that this medium should be clumpy. The size of each clump has to be $r_s \lesssim N_{\rm H}/n \lesssim 5 \times 10^{12}/n_9$ cm, and the fraction of volume occupied by this medium (i.e., the filling factor) $f_V = N_{\rm H}/(nR) = 5 \times 10^{-6}/n_9 R_{18}$. Finally, we note that the size of a clump is much smaller than the zone of the fireball visible at the time of the observation, $\approx 10^{15}/\Gamma_b$ cm, where $\Gamma_b \approx 2$–10 is the Lorentz factor of the fireball in the afterglow phase. We therefore require that most of the source is covered by these clouds, i.e., that the covering fraction $f_{\rm cov} = f_V(R/r_c) \approx 1$. This condition is satisfied when $r_s \approx 5 \times 10^{12}/n_9$ cm. The total mass contained in these clouds is $M_c \approx 3 R_{18}^3 f_{V,-6} n_9 \ M_\odot$.

It is well known from observations and models (Balsara, Ward-Thompson, & Crutcher 2001; Ward-Thompson et al. 1994) that the medium in star-forming molecular clouds is clumpy, with dense clouds or filaments embedded in a much less dense intercloud medium. The largest densities are of the order of $\approx 10^7$ cm^{-3} (Nummelin et al. 2000), i.e., lower than required. However, both observations and modeling are limited in resolution to structures of size $\gtrsim 10^{16}$ cm and would then miss smaller and higher density fluctuations. Furthermore, the total mass of the X-ray–absorbing clouds is a tiny fraction ($\approx 10^{-4}$) of the mass of a GMC ($\approx 10^5$–10^6 $M_\odot$). Prima facie, those structures could then be the tail in the power spectrum of density fluctuations in star-forming regions. Interestingly, Lamb (2001) has also stressed the role of a *dusty* clumpy medium in the GMC with regard to optical properties of GRBs. A more detailed discussion is beyond the scope of this paper.

It is worth noting that the density of this medium is similar to that of the gas responsible for iron features (e.g., Piro et al. 1999, 2000; Amati et al. 2000). This gas lies much closer to the burst and is therefore highly ionized. Interestingly, in the afterglow of GRB 000210, we find a very marginal evidence of a recombination edge by H-like Fe atoms (at a confidence level of 97%). The rest-frame energy of this feature is at 9.28 keV, corresponding, at $z = 0.85$, to $E = 5$ keV, where *BeppoSAX* data show some residual (Fig. 4). The EW $= 1 \pm 0.7$ keV is similar to that observed in GRB 991216 (Piro et al. 2000) and in the other dark GRB 970828 (Yoshida et al. 2001). This feature is the result of electron recombination on H-like Fe atoms and should be accompanied by a Kα line at 6.9 keV with a similar intensity (Piro et al. 2000). Within the errors, the upper limit EW < 0.5 keV to the latter line is consistent with this prediction.

3.2.2. *ISM Absorption in the Host Galaxy*

We now discuss the hypothesis that the absorption does not take place in the circumburst environment of the GRB, but in the interstellar medium (ISM) of the host galaxy. We find that this scenario can easily account for the properties of this burst. In fact, it immediately explains the absence of ionization features in the X-ray absorber and a dust-to-gas ratio consistent with that in our Galaxy. The typical column density through a GMC is about 10^{22} cm^{-2} (Solomon et al. 1987), and therefore even a single GMC in the line of sight could provide the necessary absorption both in the optical and in X-rays. This scenario is also consistent with the location of the GRB, which lies within $\approx$10 kpc from the center of the Galaxy.

Could nonlocal ISM absorption by the host galaxy be the unique origin of the whole population of dark GRBs? Let us first assume that GRBs occur in the disk of a galaxy similar to ours at a typical distance of 10 kpc from the center. This assumption is consistent with the *visible* properties of GRB host galaxies and the distribution of GRB offsets with respect to the host center (Bloom et al. 2002). The line-of-sight column density of interstellar hydrogen gas measured from our location in the Galaxy (10 kpc from the center) is consistent with that required to make a GRB dark ($N_{\rm H} \gtrsim 5 \times 10^{21}$ cm^{-2}) in a belt of about $\pm 5^\circ$ along the plane of the Galaxy (Dickey & Lockman 1990). Thus, of the entire population of GRBs occurring in the disk of galaxies randomly oriented in the sky, only $\lesssim$10% would be dark, much below the observed fraction of 50%–60%. Therefore, while this hypothesis can account for a fraction of dark GRBs, including this one, in order to make up the entire population of dark events, GRB host galaxies should contain quantities of dust and gas, associated with *obscured* star-forming regions, much larger than a typical galaxy like ours.

3.2.3. *Implications for the Absorber in the High-z Scenario*

Finally, given the modest a posteriori probability, we have to consider the possibility that the association of GRB 000210 with the galaxy is coincidental and that this GRB is located at $z \gtrsim 5$. In this case, the X-ray absorber of GRB 000210 is thicker, and it also can be much more ionized. For example, at $z = 5$, $\xi \lesssim 10^3$, i.e., the data are consistent with an absorber from neutral to highly ionized. In particular, we have satisfactorily fitted the data with either a neutral absorber ($\xi = 0$), which requires $N_{\rm H} = 9 \times 10^{22}$ cm^{-2}, or an ionized absorber ($\xi = 400$), which gives $N_{\rm H} = 16 \times 10^{22}$

cm^{-2}. Such values of column densities are much higher than those observed in X-ray afterglows of GRBs with optical transients (e.g., Piro et al. 2001; in 't Zand et al. 2001).

4. CONCLUSIONS

In this paper, we present the results of multiwavelength observations of GRB 000210. This event was the brightest ever observed in gamma rays in the *BeppoSAX* GRBM and WFC. Nonetheless, no optical counterpart was found down to a limit of $R = 23.5$. GRB 000210 is therefore one of the events classified as dark GRBs, a class that makes up $\approx 50\%$ of all GRBs. It is still unclear whether this class derives from a single origin or is due to a combination of different causes. Some of these GRBs could be intrinsically faint events, but this fraction should not be very high, because the majority of dark GRBs shows the presence of an X-ray afterglow similar to that observed in GRBs with optical afterglows (Piro 2001; Lazzati et al. 2002). The most compelling hypotheses to explain the origin of dark bursts involve absorption, occurring either in the local environment of the GRB (circumburst or interstellar) or as Lyα forest absorption for those bursts that have $z \gtrsim 5$.

As in the majority of bursts, GRB 000210 had an X-ray afterglow that was observed with *BeppoSAX* and *Chandra*. The temporal behavior is well described by a power law, with a decay index $\alpha_X = 1.38 \pm 0.03$, similar to that observed in several other events (e.g., Piro 2001). We did not find evidence for breaks in the light curve. The spectral index of the power law is also typical ($\Gamma = 1.95 \pm 0.15$).

Thanks to the arcsecond localization provided by *Chandra*, we identified the likely host galaxy of this burst, determined its redshift ($z = 0.846$), and detected a radio afterglow. The properties of the X-ray afterglow allowed us to determine the amount of dust obscuration required to make the optical afterglow undetectable ($A_R \gtrsim 2$). The X-ray spectrum shows significant evidence of absorption by neutral gas [$N_{H,X} = (0.5 \pm 0.1) \times 10^{22}$ cm^{-2}]. However, we do not find evidence of a partially ionized absorber expected if the absorption takes place in a giant molecular cloud, as recently suggested to explain the properties of the dark GRBs (e.g., Reichart & Yost 2001). We conclude that if the gas is local to the GRB, it has to be condensed in dense ($n \gtrsim 10^9$ cm^{-3}) clouds. We propose that these clouds represent the small-scale high-density fluctuations of the clumpy medium of star-forming GMCs.

Both the amount of dust required to extinguish the optical flux and the dust-to-gas ratio are consistent with those observed across the plane of our Galaxy. We cannot therefore exclude that the absorption takes place in the line of sight through the interstellar medium of the host, rather than being produced by a GMC embedding the burst. This hypothesis is also consistent with the location of GRB 000210 with respect to the center of the likely host galaxy. To explain the whole population of dark GRBs, this hypothesis would require that host galaxies of GRBs should be characterized by quantities of dust and gas much larger than typical, arguing again for a physical connection between GRBs and star-forming regions.

Finally, we discussed the possibility that the galaxy is unrelated to GRB 000210 and that it is a dark burst because it lies at $z \gtrsim 5$. In this case, the X-ray–absorbing medium should be substantially thicker than that observed in GRBs with optical afterglows. Assuming that GRB 000210 is a typical representative of a population of events at high redshift, then these GRBs are embedded in a much denser environment than that of closer events.

Whichever of the explanations apply, it is clear that dark GRBs provide a powerful tool to probe their formation sites and possibly to explore the process of star formation in the universe. We have at hand several observational tools to pursue this investigation. By increasing the number of arcsecond locations by radio, X-ray, and far-infrared observations, we can build up a sample of host galaxies of dark GRBs and study their distances and physical properties. The origin of the absorption in X-rays and optical can be addressed by broadband spectra and modeling, providing information on the dust and gas content of the absorbing structures. X-ray measurements are particularly promising in this respect for several reasons. First, X-rays do not suffer from absorption; in fact, roughly the same number of dark GRBs and GRBs with optical afterglows have an X-ray afterglow. Detection of X-ray lines can thus provide a direct measurement of the redshift. A comparative study of the X-ray properties of these two classes should also underline differences that can be linked to their origin, like the brightness of X-ray afterglows and the amount of X-ray absorption. Finally, measurements of variability of the X-ray–absorbing gas would provide strong support to the local absorption scenario. There are several mechanisms that can produce such a variability. The hard photon flux from the GRB and its afterglow will ionize the circumburst gas on short timescales, thus decreasing the effective optical depth with time (Perna & Loeb 1998). The detection of a transient iron edge in GRB 990705 (Amati et al. 2000) and the decrease of the column density from the prompt to the afterglow phases in GRB 980329 (Frontera et al. 2000) and GRB 010222 (in 't Zand et al. 2001) are both consistent with this scenario.

The variable size of the observable fireball that increases with the inverse of the bulk Lorentz factor can also produce variations of the column density, if the medium surrounding the source is not homogeneous. In this regard, two X-ray afterglows show some, admittedly marginal, evidence of variability of N_H (Piro et al. 1999; Yoshida et al. 2001). In conclusion, the future of the investigations of *dark* GRBs looks particularly bright.

BeppoSAX is a program of the Italian space agency Agenzia Spaziale Italiana (ASI), with participation of the Dutch space agency Nederlands Instituut voor Vliegtuigontwikkeling en Ruimtevaart (NIVR). We would like to thank H. Tananbaum and the *Chandra* team, as well as E. Costa, M. Feroci, J. Heise, and the other members of the *BeppoSAX* team, for their support in performing the observations with these satellites, and an anonymous referee for useful suggestions. G. G. acknowledges support under NASA grant G00-1010X. M. R. G. acknowledges support under NASA contract NAG8-39073 to the *Chandra* X-Ray Center. Part of the optical observations are based on observations made with the Danish 1.54 m telescope at ESO, La Silla, Chile. This research was supported by the Danish Natural Science Research Council through its Centre for Ground-based Observational Astronomy. Based in part on observations made with the Nordic Optical Telescope, jointly operated on the island of La Palma by Denmark, Finland, Iceland, Norway, and Sweden, in the Spanish Observatorio del

Roque de los Muchachos of the Instituto de Astrofísica de Canarias. Some of the data presented here have been taken using ALFOSC, which is owned by the Instituto de Astroísica de Andalucía (IAA) and operated at the Nordic Optical Telescope under an agreement between IAA and the NBIfAFG of the Astronomical Observatory of Copenhagen. Partially based on ESO VLT programme 66.A-0386(A), Cerro Paranal, Chile.

REFERENCES

Amati, L., et al. 2000, Science, 290, 953
Antonelli, L. A., et al. 2000, ApJ, 545, L39
Balsara, D., Ward-Thompson, D., & Crutcher, R. M. 2001, MNRAS, 327, 715
Bloom, J. S., Kulkarni, S. R., & Djorgovski, S. G. 2002, AJ, 123, 1111
Bloom, J. S., et al. 1999, Nature, 401, 453
Boettcher, M., Dermer, C. D., Crider, A. W., & Liang, E. P. 1999, A&A, 343, 111
Costa, E., et al. 2000, GCN Circ. 542 (http://gcn.gsfc.nasa.gov/gcn/gcn3/542.gcn3)
Dickey, J. M., & Lockman, F. J. 1990, ARA&A, 28, 215
Djorgovski, S. G., Frail, D. A., Kulkarni, S. R., Bloom, J. S., Odewahn, S. C., & Dierks, A. 2001, ApJ, 562, 654
Draine, B. T. 2000, ApJ, 532, 273
Feroci, M., et al. 2001, A&A, 378, 441
Frail, D. A., et al. 1999, ApJ, 525, L81
———. 2000, in AIP Conf. Proc. 526, 5th Huntsville Symp. on Gamma-Ray Bursts, ed. R. M. Kippen, R. S. Mallozzi, & G. J. Fishman (New York: AIP), 298
———. 2001, ApJ, 562, L55
Frontera, F., et al. 2000, ApJS, 127, 59
———. 2001, ApJ, 550, L47
Fruchter, A., et al. 2002, GCN Circ. 1268 (http://gcn.gsfc.nasa.gov/gcn/gcn3/1268.gcn3)
Fruchter, A. S. 1999, ApJ, 512, L1
Fruchter, A. S., Krolik, J. H., & Rhoads, J. E. 2001, ApJ, 563, 597
Fynbo, J. U., et al. 2001, A&A, 369, 373
Galama, T. J., & Wijers, R. A. M. J. 2001, ApJ, 549, L209
Gandolfi, G., et al. 2000a, GCN Circ. 538 (http://gcn.gsfc.nasa.gov/gcn/gcn3/538.gcn3)
———. 2000b, GCN Circ. 539 (http://gcn.gsfc.nasa.gov/gcn/gcn3/539.gcn3)
Garcia, M., Garmire, G., & Piro, L. 2000a, GCN Circ. 548 (http://gcn.gsfc.nasa.gov/gcn/gcn3/548.gcn3)
Garcia, M., Piro, L., Garmire, G., & Nichols, J. 2000b, GCN Circ. 544 (http://gcn.gsfc.nasa.gov/gcn/gcn3/544.gcn3)
Garmire, G., Piro, L., Stratta, G., Garcia, M., & Nichols, J. 2000, GCN Circ. 782 (http://gcn.gsfc.nasa.gov/gcn/gcn3/782.gcn3)
Goodman, J. 1997, NewA, 2, 449
Gorosabel, J., et al. 2000, GCN Circ. 545 (http://gcn.gsfc.nasa.gov/gcn/gcn3/545.gcn3)
Greiner, J., Schwarz, R., Englhauser, J., Groot, P. J., & Galama, T. J. 1997, IAU Circ. 6757
Groot, P. J., et al. 1998, ApJ, 493, L27
Heise, J., in't Zand, J., Kippen, M., & Woods, P. 2001, in Gamma-Ray Bursts in the Afterglow Era, ed. E. Costa, F. Frontera, & J. Hjorth (Berlin: Springer), 16
Hogg, D., et al. 1997, MNRAS, 288, 404
Hurley, K., Feroci, M., Preger, B., Cline, T., & Mazets, E. 2000, GCN Circ. 543 (http://gcn.gsfc.nasa.gov/gcn/gcn3/543.gcn3)
Im, M. I., Casertano, S., Griffiths, R. E., Ratnatunga, K. U., & Tyson, J. A. 1995, ApJ, 441, 494
in 't Zand, J., et al. 2001, ApJ, 559, 710
Jaunsen, A. O., et al. 2002, A&A, submitted (astro-ph/0204278)
Kennicutt, R. C. 1998, ARA&A, 36, 189
Kippen, R. M., et al. 2000, GCN Circ. 549 (http://gcn.gsfc.nasa.gov/gcn/gcn3/549.gcn3)
Koo, D. C., & Kron, R. G. 1992, ARA&A, 30, 613
Kulkarni, S. R., et al. 1999, ApJ, 522, L97
Lamb, D. Q. 2001, in Gamma-Ray Bursts in the Afterglow Era, ed. E. Costa, F. Frontera, & J. Hjorth (Berlin: Springer), 297
Lamb, D. Q., & Reichart, D. E. 2000, ApJ, 536, 1
Lazzati, D., Covino, S., & Ghisellini, G. 2002, MNRAS, 330, 583
Lazzati, D., & Perna, R. 2002, MNRAS, 330, 383
Madau, P. 1995, ApJ, 441, 18
Nummelin, A., et al. 2000, ApJS, 128, 213
Odewhan, S. C., Windhorst, R. A., Driver, S. P., & Kee, W. C. 1996, ApJ, 472, L13
Odewahn, S. C., et al. 1997, IAU Circ. 6735
Paczyński, B. 1998, ApJ, 494, L45
Paerels, F., Kuulkers, E., Heise, J., & Liedahl, D. A. 2000, ApJ, 535, L25
Panaitescu, A., & Kumar, P. 2001, ApJ, 554, 667
Perna, R., & Loeb, A. 1998, ApJ, 501, 467
Pian, E., et al. 2001, A&A, 372, 456
Piran, T., Kumar, P., Panaitescu, A., & Piro, L. 2001, ApJ, 560, L167
Piro, L. 2001, in Gamma-Ray Bursts in the Afterglow Era, ed. E. Costa, F. Frontera, & J. Hjorth (Berlin: Springer), 97
Piro, L., et al. 1999, ApJ, 514, L73
———. 2000, Science, 290, 955
———. 2001, ApJ, 558, 442
Predehl, P., & Schmitt, J. H. M. M. 1995, A&A, 293, 889
Reichart, D. E. 2001a, ApJ, 553, 235
———. 2001b, ApJ, submitted (astro-ph/0107546)
Reichart, D. E., & Price, P. A. 2002, ApJ, 565, 174
Reichart, D. E., & Yost, S. A. 2001, ApJ, submitted (astro-ph/0107545)
Sari, R., & Piran, T. 1999, ApJ, 520, 641
Sari, R., Piran, T., & Narayan, R. 1998, ApJ, 497, L17
Schechter, P. 1976, ApJ, 203, 297
Solomon, P. M., Rivolo, A. R., Barrett, J., & Yahil, A. 1987, ApJ, 319, 730
Stornelli, M., et al. 2000, GCN Circ. 540 (http://gcn.gsfc.nasa.gov/gcn/gcn3/540.gcn3)
Taylor, G. B., Bloom, J. S., Frail, D. A., Kulkarni, S. R., Djorgovski, S. G., & Jacoby, B. A. 2000, ApJ, 537, L17
Ward-Thompson, D., Scott, P. F., Hills, R. E., & Andre, P. 1994, MNRAS, 268, 276
Waxman, E., & Draine, B. T. 2000, ApJ, 537, 796
Waxman, E., Kulkarni, S. R., & Frail, D. A. 1998, ApJ, 497, 288
Yoshida, A., Yonetoku, N. M., Murakami, T., Otani, C., Kawai, N., Ueda, Y., Shibata, R., & Uno, S. 2001, ApJ, 557, L27